Title: More than germ cells: vascular development in the early zebrafish (*Danio rerio*) gonad

Authors: Michelle E. Kossack[1†], Lucy Tian[1], Kealyn Bowie[2], Jessica S. Plavicki[1*‡]

[1] Pathology and Laboratory Medicine Department, Brown University, Providence, RI

[2] Department of Ecology, Evolution, and Organismal Biology, Brown University, Providence, RI

* Corresponding Author: jessica_plavicki@brown.edu, 70 Ship St, Box G-E5, Providence, RI, 02903

[†] Supported by F32ES023650 and 5T32ES007272 both from NIEHS

[‡] Supported by NIEHS K99/R00 (ES023848), a CPVB Phase II COBRE (2PG20GM103652), and an NIEHS ONES award (ES030109)

Running Title: Vascular development in the early zebrafish gonad

Keywords: Zebrafish, bipotential gonad, endothelial, lymphatic, pericyte, macrophage, reproduction, single-cell, vasculature

Summary Sentence:

Delineating the complex cellular interactions between vascular and lymphatic endothelial cells, pericytes, and macrophage in the bipotential gonad is essential for understanding the differentiation and functioning of the mature gonad.

Abstract: Zebrafish are routinely used to model reproductive development, function, and disease, yet we still lack an understanding of the fundamental steps that occur during early bipotential gonad development, including when stromal cells invade the bipotential gonad to support gonad growth and differentiation. Here, we use a combination of transgenic reporters

and single-cell sequencing analyses to define the arrival of different stromal cell types to the larval zebrafish gonad. We determined that blood arrives to the gonad via the gonadal artery, which is derived from the swim bladder artery. We find that vascular and lymphatic development occurs concurrently in the bipotential gonad and our data suggest that, similar to what has been observed in developing zebrafish embryo, lymphatic endothelial cells can be derived from vascular endothelial cells. Although we established that *pdgfrb* expression is not exclusive to ovarian pericytes, we can resolve that *pdgfrb*+ pericytes support the migration of endothelial tip cells within the ovary. We observed that macrophage are the first stromal cell type to populate the zebrafish gonad, establishing a nascent resident population as early as 12 dpf. Further, macrophage are responsible for removing cellular material, particularly during sex differentiation. This foundational information demonstrates that the early bipotential gonad contains complex cellular interactions which may shape the health and function of the later gonad.

Introduction:

The developmental basis of the adult disease hypothesis postulates that the origins of some disease can be traced back to developmental changes, sometimes very subtle, that produce long-term cascading effects to ultimately alter organ function and health (1). Given their genetic similarity to humans, zebrafish have been extensively used to model early embryonic development (2). More recently zebrafish have also been used to model juvenile development and adult health, including gonadal formation and fertility (3–5).

The zebrafish gonad undergoes the same developmental stages as mammals; however, the timeline is elongated. The protracted developmental timeline allows for a detailed examination of very early periods of gonadal development, which have been understudied and may be sensitive to genetic and environmental disruptions. In mammals, primordial germ cells form at 7 days post conception (dpc) and, between ~9.5 and ~11.5 dpc, migrate from the

hindgut to the urogenital ridge (6–8). In mice, the primary sex-determining gene, *sex determining region Y* (*Sry*), must be activated before 11 dpc to initiate the transition from a bipotential gonad to a testicular development program (9). Since the mammalian bipotential period only lasts <2 days, it can be difficult to investigate early sources of reproductive disease that could occur during this critical developmental stage.

In the zebrafish, germ cells are specified at 4 hours post-fertilization (10). However, the primordial germ cells (PGCs) remains quiescent while migrating into a position ventral to the hind gut, a process which occurs from 1 day post-fertilization (dpf) to approximately 10 dpf (see (11) for a detailed review). From 10 dpf until approximately 20 dpf, most of the germ cells undergo mitosis, initiate meiosis, and remain in a bipotential state. Males and females maintain a population of germline stem cells, which allow both sexes to produce new gametes throughout their life. Zebrafish do not have a primary sex chromosome. Instead, during the biopotential period, early-stage oocytes produce paracrine signals, which further support the development of primary and secondary female sex characteristics (12,13). Around 20 dpf, in the presence of sufficient oocyte-derived signaling, the oocytes continue to mature, growing larger, and, ultimately, forming an ovary. In the absence of sufficient oocyte-derived signaling, oocytes undergo apoptosis and the gonad will progress with a testicular developmental program (14,15). Somatic cells receive germ cell-derived signals and respond by producing sex-specific factors that further shape sexual differentiation (16). Somatic cells are shown in close association with primordial germ cells as early as 4 dpf (17). By 11 dpf, these somatic cells have formed a bilayer and begin to express sex specific markers (16). However, outside of these studies nothing is known about the presents of other cell types at the biopotential gonad.

In mammals, a major area of research has been to delineate the role of support and steroidogenic cells in sex determination and gonad maturation. Comparatively less has been done to investigate the role of stromal cells (i.e., non-germ, non-support, and non-steroidogenic cells) in the developing bipotential and differentiated mammalian gonad. Some research

indicates that additional cell types are present at early stages of gonad development. De Falco et al. (18) found that macrophage are present at the urogenital ridge at E10.5, just prior to sex determination, and that macrophage depletion limits vascular development. Brennan et al. (19) found that, in contrast to previous ideas about the timeline of vascular development in the mouse gonad, endothelial cells in XX and XY individuals are present by 11.5 dpc and form lumenized vessels that are perfused with blood. The authors went on to show that vessel formation is essential for testis development; however, considerably less is known about the dynamics of vascular and other stromal cell development in the ovary. Recently, Garcia-Alonso et al., (20) performed single-cell sequencing of the mouse gonad at 10.5 dpc and found many different stromal cell types are present including vascular and lymphatic endothelium, macrophage, and pericytes. Together, the presence of many different cell types suggests that bipotential gonad health and later ovary and testis function may rely on complex interactions between germ cells and stromal cells during the bipotential phase.

While it is known that the mature zebrafish ovary and testis contain endothelial and lymphatic vasculature as well as perivascular cells and macrophage (21), the developmental timeline for the arrival of these cell types to the developing gonad has not previously been described. The long bipotential period of gonadal development in zebrafish compared to mice provides an excellent opportunity to thoroughly assess the arrival of stromal cells prior to sex determination. Using transgenic zebrafish with fluorescently expressed cellular markers, we tracked the arrival of stromal cells to the bipotential zebrafish gonad. We found that the bipotential gonad is more complex than originally considered, which suggests that additional cell types have the potential to contribute to gonad development, sex determination, and fertility.

Material and Methods:

Zebrafish Rearing: Zebrafish (*Danio rerio*) were raised as described in Kossack et al. and Westerfield (22,23). Larvae were placed in tanks at 5 dpf in 100mL rotifer culture, 400mL of fish

105 water static, and one drop of RG Complete (Reef Nutrition). From 5 to10 dpf, larvae were fed
106 GEMMA Micro 75 (Skretting Zebrafish©) twice a day and live rotifers once a day. At 10 dpf,
107 water flow was started as a slow drip, approximately one drop a second. From 10-20 dpf, fish
108 were fed GEMMA Micro 75 twice a day, along with rotifers and artemia once a day. From 21 to
109 28 dpf, the water flow rate was increased until a standard flow rate was established. The fish
110 were treated as adults at 90 dpf and fed GEMMA Micro 300 once a day.
111 Juvenile fish were euthanized according to procedures approved by the Institutional
112 Animal Care and Use Committee at Brown University and adhered to the National Institutes of
113 Health "Guide for the Care and Use of Laboratory Animals". In short, fish were placed in 0.04%
114 MS-222 solution for 10-15 mins followed by ice water for 20 mins at which point they were
115 decapitated and placed in 4% PFA overnight.
116 In establishing the developmental timeline, we measured the standard length of fish. The
117 standard length is correlated with developmental stage during these ages (24,25). The full list of
118 replicates, individuals, average length, and observations can be found in **Supplemental Table**
119 **S1.**
120
121 *Transgenic lines utilized*: To mark vascular endothelial cells (VECs) we used three transgenic
122 lines, *Tg(fli1:nEGFP)*^{y7}*, Tg(kdrl:GFP)* originally *Tg(flk1:GFP)*^{la116}*,* and *Tg(kdrl:DsRed2)* (26–28).
123 Lymphatic endothelial cells (LECs) were labeled with *Tg(mrc1a:EGFP)* and *Tg(-*
124 *5.2lyve1b:DsRed) (29,30)*. *Tg(piwil1:EGFP)* originally Tg(ziwi:EGFP) marked germ cells, and
125 *TgBAC(pdgfrb:EGFP)* marked perivascular cells (31,32). In the study of macrophage we utilized
126 *Tg(mpeg1:EGFP), Tg(mpeg1:Gal4FF)gl25,* and *Tg(UAS:Kaede)* (33,34). For readability and
127 simplicity, we will refer to these transgenic lines by the simplified notations inside the
128 parentheses, i.e *Tg(-5.2lyve1b:DsRed*) is listed as *lyve1b:DsRed*.
129

Antibody Staining: Antibody staining for germ cell protein Vasa was performed as described in Leerberg et al. (16) using anti-Vasa antibody from GeneTex (GTX1238306) at a working concentration of 1:1000. All secondary antibodies were used at 1:500 and are as follows: goat anti-rabbit IgG 488 (Thermo Fisher Scientific Cat# A-11034, RRID:AB_2576217) and goat anti-rabbit IgG 633 (Thermo Fisher Scientific Cat# A-21071, RRID:AB_2535732). After protein labeling, tissues were stained with Hoechst 33342 (Invitrogen H3570) at a concentration of 1:10,000 overnight, dissected, and placed in Vectashield mounting media (Fisher Scientific, NC9265087) for subsequent imaging.

Photoconversion and live imaging: Double transgenic line *mpeg1:GAL4;UAS:Kaede* fish were identified at 3 dpf. At 12 dpf, fish were anesthetized in 0.02% MS222 for 1 minute then mounted on a 35mm glass bottom microwell dish (MatTek, Part No. P35G-1.5-14-C) in 2% low-melting temperature agarose (Fisher Scientific, bp1360-100) made in egg water (4 parts per thousand salt). The mounted fish was surrounded in 0.02% MS-222 and placed on the confocal microscope. Using 20x objective, the mid-section of the fish was exposed to full-power LED 405nm fluorescent light for 60 seconds to photoconvert the Kaede from green to red. The fish was immediately removed from agarose and replaced in the tank. The tank was covered with foil to protect the fish from additional light during transportation back to the fish facility. 24 hours later, the fish were again anesthetized and mounted laterally in agarose. Using a 20x objective, *piwil1:EGFP* expressing fish were identified from the previously photo-converted fish and imaged.

Imaging: Images were collected on a Zeiss LSM 880 confocal microscope. Maximum intensity projections, orthogonal slices, and colocalization analysis were performed with ZenBlack (Zeiss). Tissues from 10 – 15 dpf zebrafish were mounted on Premium microscope slides (Fisher Scientific, 12-544-7) with Premium cover glass (Fisher Scientific,12-548-B) held in place

by vacuum grease. Tissues >20 dpf were mounted in 1% low-melting agarose in a 35mm glass bottom microwell dish.

Sequencing Analysis: From Liu et al., (21) we obtained matrixes of gene and feature count. These large matrixes gathered from raw single-cell sequencing data display individual cells on one axis vs. counts of every gene detected in the other. From this data we are able to perform principal component analysis to group similar cells together, which is referred to as clustering. For more details about the analysis see Seurat (35,36), and R code (https://repository.library.brown.edu/studio/item/bdr:d4ef3vpa/). Clustering of the ovarian cells was performed as described in Liu et al. and cluster 5 was identified as the "Blood Vessel" cluster as described in the publication (21). We isolated this group using the subset() function and looked at the expression of VEC and LEC markers. We attempted sub-clustering analysis, but there were insufficient cell numbers within this cluster alone to draw meaningful information.

To generate the pericyte Venn diagram, we used publicly available data from Liu et al. and Shih et al. (21,37). Briefly, both publications included lists of highly expressed genes identified in all cell type. We, therefore, were able to download the list of genes expressed in the cell types of interest, filter them for expression level, and compare the lists. From Liu et al. (21), we downloaded the dataset of differentially expressed genes in stromal cells (from Supplemental Table 5) and filtered the data to only include genes whose p_val_adj<0.05. We called this group "ovarian stromal cells". We applied the same filtering parameters to narrow down the "ovarian pericytes" (sub-cluster 2). We eliminated duplicates within each list to generate 2,606 genes in the ovarian stromal cell group and 441 genes in the ovarian pericyte group.

Similarly, using publicly available data from Shih et al. (37), we downloaded the highly expressed genes identified in all pdgfrb-expressing cells (from Supplemental Table S2.1). As described in the publication we filtered for expression level $\log_2>1$, this list of genes was defined

as "*pdgfrb*+ cells". We performed the same methodology to Table S1.4, which was identified as "cluster 39". We eliminated duplicates within each list, which resulted in 2,084 genes in *pdgfrb*+ cells and 105 genes in cluster 39. Using the list comparison tool (https://rnact.crg.eu/compare), we found the overlapping and unique genes for each group. These numbers were used to create the Venn diagram using Venn.Plot in R studio. List details are available in **Supplemental Table S2**.

Results:

Vascular endothelial cells make initial contact with the anterior gonad

To establish a timeline of vascular development in the gonad, we used a double transgenic line *kdrl:DsRed; fli1:nEGFP* that carries both the pan-endothelial marker *fli1:nEGFP* as well as *kdrl:DsRed*, which marks vascular endothelial cells (VECs). Beginning at 10 dpf, we used a qualitative scale to measure the distance between the gonad, marked by germ cells, and the VECs. We defined the relationship between the cells using three categories, "No Contact" (**Figure 1A**), "Proximal" (near, but not physically associated, **Figure 1B**), or "Contact" (**Figure 1D, Supplemental Figure S1**). We found that in most individuals (n=15/17), VEC contact with the germ cells occurred by approximately 20 dpf (**Figure 1F**), which corresponded to a standard length of 7.21± 0.666mm (**Figure 1G, Supplemental Table S1**). We observed that the initial VECs contact occurred with the anterior most portion of the developing gonad (**Figure 1E**). Prior to this study, it was not known which vessels supplied blood to the bipotential gonad. We determined that at 20 dpf the blood supply to the bipotential gonad originates from the swim bladder artery (**Figure 1H**). Posterior to the anterior chamber of the swim bladder, the swim bladder artery divides, with two different branches supplying blood to the right and left gonad (**Figure 1H**). We termed this artery the gonadal artery.

Specification of lymphatic endothelial cells in the gonad resembles embryonic lymphatic development

The role of the lymphatic vasculature in organogenesis and homeostasis has been understudied in zebrafish (38). Recent single-cell sequencing of the zebrafish ovary found that lymphatic endothelial cells (LECs) are present in the ovary by 40 dpf (21); however, it is not known when lymphatic cells invade the ovary and create functional networks within it. To determine when VECs and LECs reach the ovary, we visualized the endothelium by crossing canonical vascular endothelial reporter lines *kdrl:GFP* or *kdrl:DsRed* with established lymphatic endothelial transgenic reporters, *mrc1a:EGFP* or *lyve1b:DsRed* (29). Using this double transgenic approach, we determine that LECs are detected in the gonad at 20 dpf, the same time as VECs (**Figure 2A, 2B,** 20 dpf, standard length of 7.17±1.04mm, n=13/13, **Supplemental Table S1**).

It is unclear from our analysis of early stromal colonization of the gonad if VECs give rise to LECs or if the lymphatic endothelium enters the gonad independent of the vascular endothelium. During embryonic development, LECs are derived from venous VECs (30,39–46). *flt4*, a marker of venous endothelial cells and LECs, is required for initiating LEC development. Expression of *flt4* is followed by the expression of *prox1a*, which specifies the lymphatic fate in mammals (46–53). However, in other contexts, such as anal fin vascularization, VECs are derived from LECs (52). To gain insight into which mechanism might be utilized in the gonad, we mined previously available single-cell sequencing from the 40 dpf zebrafish ovary (21). We sub-clustered the vasculature (“Blood Vessels”) and looked for expression and co-localization of specific endothelial markers. We found VEC markers *kdrl*, *fli1*, and *flt1*, to be expressed in the majority of cells (**Figure 3A**) whereas *lyve1b*, *flt4*, and *prox1a* were expressed in a smaller subset of cells (**Figure 3B**). Next, we assessed whether *kdrl* and *lyve1b* were co-expressed in this cluster and we found no overlap in expression (**Figure 3C**). However, *lyve1b* was co-expressed with the venous marker *flt4*, suggesting that lymphatic development in the gonad

may occur in a manner similar to what has been observed in the embryonic endothelium (29). We note that we were not able to examine the expression of *mrc1a* in the single-cell sequencing data set because it was not detected in the original sequencing analysis.

To assess if LECs were derived from VECs in the bipotential gonad, we used confocal microscopy to image 20 dpf gonads expressing transgenic markers for both VECs and LECs (*kdrl:DsRed; mrc1a:EGFP*). Our imaging revealed overlap in the *kdrl:DsRed* and *mrc1a:EGFP* expression domains (**Figure 4A**). However, in most of the cells that expressed both genes, the level of transgenic expression was not equal, and we consistently observed expression of one marker being dominant over the other in the maximum intensity projection (**Figure 4B and 4C**). Orthogonal slices of the z-stacked images illustrate that the incongruent levels of expression between markers is not an artifact of the maximum intensity projection (**Figure 4D**). Finally, we used Zen Black to perform a co-localization analysis of the confocal images and found that although the *mrc1a:*EGFP expression obscured the visibility of the *kdrl:DsRed*, there was 100% overlap in signal (**Figure 4E,** Overlap coefficient = 0.97). Together this supports that LECs in the 20 dpf zebrafish gonad are derived from VECs, and as lymphatic specific expression increases, vascular endothelial expression decreases.

Pdgfrb+ perivascular cells associate with vascular tip cells invading the bipotential gonad

Pericytes are a sub-type of mural cells that have since their discovery been difficult to clearly distinguish from other perivascular cell types (54). In the developing zebrafish embryo, pericytes were originally defined by expression of *pdgfrb*, their morphology, and their positional relationship to the vasculature. However, recent evidence from embryonic zebrafish indicates that while pericytes tend to have the highest *pdgfrb* expression they constitute only a subset of the *pdgfrb*:EGFP+ cells (37). Similarly, single-cell sequencing of the ovary showed that *pdgfrb*+ cells are found in multiple clusters of stromal cells. In this larger group, pericytes were better defined by the expression of *plp1b*, a sub-cluster with high *pdgfrb* and *notch3* expression (21).

To determine if there was a pericyte marker unique to the gonad and not expressed in embryos, we compared expression of embryonic *pdgfrb*:EGFP cells and cluster 39 (highest *pdgfrb* expression (37)) with ovarian stromal cells (*pdgfrb*+ cells (21)) and ovarian pericytes (*plp1b*+ (21)). We did not identify gene expression signatures that were unique to ovarian pericytes (**Figure 5**); however, eight genes were found to be co-expressed in cluster 39, ovarian stromal cells, and ovarian pericytes (a complete list of overlap in **Supplemental Table S2**). These eight genes did not include the ovary pericyte-specific marker *plp1b*, this suggests either that ovarian pericytes have unique functions not shared by embryonic pericytes, or that the function of *plp1b* in the ovarian pericytes is not intrinsic to pericytes.

As with all vascular beds, pericytes in the ovary are an essential part of the vascular unit, creating stability for the constant vascular modeling that occurs as an inherent part of ovarian function (as reviewed in (55). Since *pdgfrb* is an imperfect marker of pericytes, we used the double transgenic *pdgfrb:EGFP;kdrl:DsRed* to determine if *pdgfrb*+ cells within the gonad were also in contact with a vessel. We found that oblong *pdgfrb*+ cells are associated with vessels in the developing gonad and based on their gene expression, position, and morphology, appeared to be pericytes. The *pdgfrb*+ presumptive pericytes arrived at the gonad along with the endothelial cells (**Figure 2A,** 20 dpf, 7.61±0.515mm, n=8/9, **Supplemental Table S1**). Confocal images revealed projections extending from *pdgfrb*+ cells between *kdrl*+ vessels (**Figure 6**), suggesting that pericytes may aid in the migration of vascular tip cells, which has been observed during the vascularization of other tissues (32,56).

Macrophage arrive at the bipotential gonad prior to other stromal cells types

Lastly, we investigated the arrival of macrophage to the gonad. Macrophage are known to play a substantial role in both ovary and testis function in mammals, however their colonization of the zebrafish gonad remains unclear (57–59). We found that while macrophage colonization of the gonad in most individuals was concurrent with vascularization of gonad, in

some cases we observed macrophage within the gonad prior to vascularization (**Figure 2A,** 12 dpf, 4.74±0.849mm, n=6/14, **Supplemental Table S1**). Notably, we found that at 20 dpf, when the gonad is undergoing sex determination, there are more macrophage present, and they can be seen engulfing germ cells (**Figure 7B,C**). This suggests that macrophage may play an active role in gonad differentiation in zebrafish.

Finally, we asked if the macrophage that make initial contact with the gonad became resident macrophage or if they were only transiently interacting with the germ cells. Given the superficial position of the macrophage in contact with the early gonad (**Figure 7A**), we hypothesized that macrophage found during the bipotential stage were not tissue-resident and the resident population would not be established until after sex determination. To test this hypothesis, we used a pan-macrophage reporter to drive expression of Kaede *(mpeg1:GAL4; UAS:Kaede)*, a photoconvertible fluorescent protein that changes from green to red following exposure to 405nm light. We exposed fish at 12 dpf to 405nm light in a defined region surrounding the gonad. As a result, macrophage in and near the gonad were converted to red, leaving the remaining macrophage in the body green. 24 hours later we used live imaging to observe the macrophage population within the gonad. The presence of only red macrophage would indicate that no new macrophage had entered the gonad and suggest that macrophage become resident prior to sexual differentiation. The presence of green macrophage in addition to red macrophage would indicate either: (1) continued colonization of the gonad, (2) the presence of transient populations of macrophage, or (3) newly divided macrophage from a previously photoconverted cell although likely some red would remain from the mother cell. We found that after 24 hours, a subset of macrophage were retained in the gonad and expressed the red photoconverted kaede protein (**Figure 7E,** red arrowhead, n=5). We also observed green macrophage in and in the proximity of the gonad (**Figure 7F,** green arrow). Finally, several cells also were green and red mixed suggesting that they had some previous conversion while generating new Kaede protein (**Figure 7D,** blue arrow). It is difficult to say

where the double-labeled cells originated. Given the ratio of green to red in these cells it is most likely that these cells were on the periphery of the conversion area and migrated to the gonad while producing new Kaede protein. Together, these data suggest that at 12 dpf, there is an early population of resident macrophage that cells within the bipotential gonad.

Discussion:

Here we provide the first report of vascularization of the early zebrafish gonad, a fundamental and understudied component of reproductive development and health. We found that vascular endothelial cells and lymphatic endothelial cells are present in the ovary by 15 dpf. In mammals, two previous studies tracked the arrival of endothelial cells to the early gonad (19,60). Both studies found that by 11.5 dpc endothelial cells, marked by Tie-2, Flt1, and PECAM, were present in the gonad. However, neither publication examined earlier time points until Garcia-Alonso et al. (20) performed single-cell sequencing on 10.5 dpc mice. In this data set, we can query markers for stromal cell types and find all are present, however, this methodology lacks spatial resolution. Based on these previous studies, we can conclude that vascularization during the bipotential phase of gonad development is very similar between zebrafish and mammals. Although our investigation clearly indicates VECs and LECs are present in the bipotential gonad, it does not evaluate when the vessels establish a functional network. Future investigations will be required to determine when the vessels are lumenized and are able to transport physiological signals and waste.

Prior mammalian studies used pan-endothelial cell markers and, therefore, these studies do not allow us to distinguish between endothelial cell types during gonad development (61,62). In adult mice, LECs and VECs have distinct domains in both the ovary and testis (19,62), but the establishment of these domains early in development is unclear. In mice, Brennen et al. (19) found that LECs, marked by $Prox1^{+/lacZ}$, are present in the mesonephros at 13.5 dpc and enter the gonad at 17.5 dpc in both sexes. However, using a transgenic Prox1-EGFP mouse,

Svingen et al. found that the ovary does not contain LEC until after birth at post-natal day 10, while the testis contains LEC by 17.5 dpc (62). Yet murine expression analysis using single-cell sequencing shows evidence of *prox1* expression in the gonad at 10.5 dpc (20). Each of these studies used different methods and criteria (lacZ, transgenic line, mRNA expression, respectively) to determine the presence of LEC in the gonad using *Prox1*. Therefore, the observed discrepancies could be due to differences in methodology or criteria. When comparing zebrafish to mice, it becomes more difficult to assess the parallels between these two model species. Most mammalian studies use *Prox1* as the LEC marker. In our study, we defined LECs to be *mrc1a* or *lyve1b* expressing cells, because *prox1* is known to be expressed in a number of different ovarian cell types and is not required for lymphatic cell specification in zebrafish (44,49). Single-cell sequencing is able to detect extremely low expression of *Mrc1* and *Lyve1* (the mammalian orthologs of mrc1a and lyve1b respectively) at 10.5 dpc, which suggests the earlier timeline of LEC arrival seen in zebrafish also occurs in mammals (20).

We also demonstrated that the *pdgfrb* expression domain within the ovary is not limited to pericytes and likely includes other mural cells with different sub-functionalizations. We show that *pdgfrb*+ cells extend between vessels within gonad, which likely reflects pericytes extending to support migrating vascular tip cells, a phenomenon that has been observed in other developmental contexts (32,56). Vascular tip cells release *pdgf* ligands which signal perivascular cells to follow and stabilize the forming vessel. When performing confocal analysis of the tissue morphology, we kept detection levels controlled to accurately represent the pericyte morphology. In this case if we overexposed the channel, we were able to see some *kdrl:DsRed* adjacent to the *pdgfrb*+ cell (data not shown). Likely we are limited by the thickness of the tissue, and strength of the DsRed fluorophore.

Pericyte biology is still relatively nascent and *pdgfrb* has been routinely used as the primary marker across species. In embryonic zebrafish, *pdgfrb* is required for the formation of the intersegmental vessels and meningeal angiogenesis (63,64). In other species, it is known

that pericytes are essential for vascular stability and reconstruction of the ovarian vasculature during follicle development and post-ovulation (65–68). Consistent with this finding, inhibition of PDGFR in the rat ovary causes hemorrhaging (69). Together, these reports indicate a role of pericytes in the function and establishment of the blood follicle barrier (70,71). When we compared the gene expression profiles of pdgrfb+ cells in cluster 39, ovarian stromal cells, and ovarian pericytes, we found that eight genes were shared between cluster 39, ovarian stromal cells, and ovarian pericytes. Of these, we noticed two were associated with cell adhesion (*pcdh1b* and *s1pr1*). *s1pr1* has been shown to play critical roles in negatively regulating angiogenesis in zebrafish (72) and knockout of S1pr1 in mice causes size-selective openings in the blood-brain barrier (73). Although it is likely that *s1pr1* is not specific to pericytes, as it is also expressed in VEC including hepatocellular carcinoma (74), the shared expression of cell adhesion genes in cluster 39 and ovarian pericytes supports the idea that pericytes play a critical role in the blood follicle barrier development in zebrafish. It will be necessary to understand how pericytes interact with the ovarian vasculature, particularly in addressing ovarian disease. Both ovarian hyperstimulation syndrome and polycystic ovary syndrome are associated with altered ovarian vasculature (75–77). Although it is well established that pericytes perform a critical role in vascularization and angiogenesis, the role that perivascular cells play in disease etiology remains unclear (reviewed in (76)). Zebrafish are able to model ovarian diseases such as PCOS (78), therefore the discovery of stromal cells in the bipotential gonad offers an opportunity to investigate the role of these cells in the very early reproductive disease formation.

We discovered that macrophage are present in the early bipotential gonad and can be seen engulfing germ cells during the bipotential phase. In mice, yolk-sac-derived macrophage are responsible for clearing cellular debris from endothelial cells, Sertoli cells and germ cells, as well as for pruning vascular networks in the testis (18). In other contexts, macrophage are known to release angiogenic cues that shape vascular development (79–83). Therefore, their

presence in the bipotential gonad prior to the arrival to VECs could suggest that macrophage could be involved in directing vascularization of the gonad. While ovarian resident macrophage are essential for folliculogenesis, ovulation, and the clearing of atretic follicles (59,84,85) and cellular debris (58), prior to this study, macrophage phagocytosis in the zebrafish ovary had not been observed. We also report that gonad resident macrophage are present by 12 dpf and the population is dynamic during this developmental window with new macrophage migrating into and out of the gonad. In mice, ovarian resident macrophages can be divided into 5 different populations. Two of these initial subpopulations are embryonically derived, one population from the yolk-sac and the other from the fetal liver (58). However, the majority of research studies have investigated resident macrophage function after sex determination. The presence of macrophage in the zebrafish bipotential gonad, suggests that macrophage may also be present in the mammalian bipotential gonad and contribute to important steps in sexual differentiation.

In conclusion, we found that stromal cells begin populating the bipotential gonad at 12 dpf. Our data suggest that VEC give rise to LEC in the gonad and create a complex network of endothelial cells by 20 dpf, however, it is still unclear when these vessels become functional conduits for physiological signals and nutrients. We found that *pdgfrb* support the migration of vascular tip cells; however, a more specific ovarian pericyte marker is needed to understand the role of pericytes vs. *pdgfrb* expressing cells in ovarian development. Finally, we found that tissue resident macrophage can be found in the gonad as early as 12 dpf and are important for clearing oocyte debris during sexual differentiation. Our foundational information regarding stromal cell invasion into the biopotential gonad contributes to the understanding of the early bipotential environment and how it may contribute to the etiology of reproductive disease.

Acknowledgments:

We would like to thank Rachel Cyr for all her meticulous work caring and raising the fish. We would also like to thank the Weinstein and Draper labs for sharing their transgenic lines that

made this study possible. Thank you to Dr. Bruce Draper and Dr. Daniel Spade for their comments on the manuscript. This work was made possible by funding from NIEHS to Dr. Michelle Kossack F32ES023650 and 5T32ES007272. Dr. Jessica Plavicki was supported by an NIEHS K99/R00 (ES023848), a CPVB Phase II COBRE (2PG20GM103652), and an NIEHS ONES award (ES030109).

Data Availability:

The data underlying this article are available in the Brown Digital Repository at: https://repository.library.brown.edu/studio/item/bdr:d4ef3vpa/

Conflict of Interest Statement:

MEK, LT, KB, and JSP have no conflicts of interest to declare.

Author Contribution:

MK: Conceptualization, methodology, investigation, writing – original draft, review, and editing, visualization. LT and KB: Investigation, writing – review and editing. JSP: Resources, writing – review and editing, supervision, project administration, fund acquisition.

References:

1. De Boo HA, Harding JE. The developmental origins of adult disease (Barker) hypothesis. Aust N Z J Obstet Gynaecol. 2006 Feb 1;46(1):4–14.

2. Howe K, Clark MD, Torroja CF, Torrance J, Berthelot C, Muffato M, et al. The zebrafish reference genome sequence and its relationship to the human genome. Nature. 2013;496(7446):498–503.

3. Baker TR, Peterson RE, Heideman W. Early Dioxin Exposure Causes Toxic Effects in Adult Zebrafish. Toxicol Sci. 2013 Sep;135(1):241–50.

4. King Heiden T, Carvan MJ, Hutz RJ. Inhibition of follicular development, vitellogenesis, and serum 17β-estradiol concentrations in zebrafish following chronic, sublethal dietary exposure to 2,3,7,8-tetrachlorodibenzo-p-dioxin. Toxicol Sci. 2006;90(2):490–9.

5. King Heiden TC, Spitsbergen J, Heideman W, Peterson RE. Persistent adverse effects on health and reproduction caused by exposure of zebrafish to 2,3,7,8-Tetrachlorodibenzo-p-dioxin during early development and gonad differentiation. Toxicol Sci. 2009;109(1):75–87.

6. Bendel–Stenzel M, Anderson R, Heasman J, Wylie C. The origin and migration of primordial germ cells in the mouse. Semin Cell Dev Biol. 1998 Aug;9(4):393–400.

7. McLaren A, Durcova-Hills G. Germ cells and pluripotent stem cells in the mouse. Reprod Fertil Dev. 2001;13(8):661.

8. Wilhelm D, Palmer S, Koopman P. Sex Determination and Gonadal Development in Mammals. Physiol Rev. 2007 Jan 1;87(1):1–28.

9. Hiramatsu R, Matoba S, Kanai-Azuma M, Tsunekawa N, Katoh-Fukui Y, Kurohmaru M, et al. A critical time window of Sry action in gonadal sex determination in mice. Development. 2009;136(1):129–38.

10. Yoon C, Kawakami K, Hopkins N. Zebrafish vasa homologue RNA is localized to the cleavage planes of 2- and 4-cell-stage embryos and is expressed in the primordial germ cells. Development. 1997;124(16):3157–65.

11. Michelle E. Kossack, Bruce W. Draper. Genetic regulation of sex determination and maintenance in zebrafish (Danio rerio). Curr Top Dev Biol. 2019;134:119–49.

12. Dranow DB, Hu K, Bird AM, Lawry ST, Adams MT, Sanchez A, et al. Bmp15 Is an Oocyte-Produced Signal Required for Maintenance of the Adult Female Sexual Phenotype in Zebrafish. Mullins MC, editor. PLOS Genet. 2016 Sep 19;12(9):e1006323.

13. Wilson CA, High SK, McCluskey BM, Amores A, Yan YL, Titus TA, et al. Wild sex in zebrafish: Loss of the natural sex determinant in domesticated strains. Vol. 198, Genetics. 2014. 1291–1308 p.

14. Dranow DB, Tucker RP, Draper BW. Germ cells are required to maintain a stable sexual phenotype in adult zebrafish. Dev Biol. 2013 Apr;376(1):43–50.

15. Takahashi H. Juvenile hermaphroditism in the zebrafish, Brachydanio rerio. Bull Fac Fish Hokkaido Univ. 1977;28(2):57–65.

16. Leerberg DM, Sano K, Draper BW. Fibroblast growth factor signaling is required for early somatic gonad development in zebrafish. Mullins MC, editor. PLOS Genet. 2017 Sep 5;13(9):e1006993.

17. Braat AK, Zandbergen T, Van De Water S, Goos HJTH, Zivkovic D. Characterization of zebrafish primordial germ cells: Morphology and early distribution of vasa RNA. Dev Dyn. 1999;216(2):153–67.

18. DeFalco T, Bhattacharya I, Williams AV, Sams DM, Capel B. Yolk-sac-derived macrophages regulate fetal testis vascularization and morphogenesis. Proc Natl Acad Sci. 2014;111(23):E2384–93.

19. Brennan J, Karl J, Capel B. Divergent Vascular Mechanisms Downstream of Sry Establish the Arterial System in the XY Gonad. Dev Biol. 2002 Apr;244(2):418–28.

20. Garcia-Alonso L, Lorenzi V, Mazzeo CI, Alves-Lopes JP, Roberts K, Sancho-Serra C, et al. Single-cell roadmap of human gonadal development. Nature. 2022 Jul 1;607(7919):540–7.

21. Liu Y, Kossack ME, McFaul ME, Christensen LN, Siebert S, Wyatt SR, et al. Single-cell transcriptome reveals insights into the development and function of the zebrafish ovary. eLife. 2022 May 19;11:e76014.

22. Westerfield M. The zebrafish book: A guide for the laboratory use of zebrafish Danio (Brachydanio) rerio. Eugene, OK: Westerfield, M; 2007.

23. Kossack ME, Manz KE, Martin NR, Pennell KD, Plavicki J. Environmentally relevant uptake, elimination, and metabolic changes following early embryonic exposure to 2,3,7,8-tetrachlorodibenzo-p-dioxin in zebrafish. Chemosphere. 2022;136723.

24. Kimmel CB, Ballard WW, Kimmel SR, Ullmann B, Schilling TF. Stages of embryonic development of the zebrafish. Dev Dyn. 1995 Jul;203(3):253–310.

25. Singleman C, Holtzman NG. Growth and maturation in the zebrafish, Danio rerio: a staging tool for teaching and research. Zebrafish. 2014/06/30 ed. 2014 Aug;11(4):396–406.

26. Roman BL, Pham VN, Lawson ND, Kulik M, Childs S, Lekven AC, et al. Disruption of acvrl1 increases endothelial cell number in zebrafish cranial vessels. Development. 2002;129(12):3009–19.

27. Choi J, Dong L, Ahn J, Dao D, Hammerschmidt M, Chen JN. FoxH1 negatively modulates flk1 gene expression and vascular formation in zebrafish. Dev Biol. 2007 Apr 15;304(2):735–44.

28. Kikuchi K, Holdway JE, Major RJ, Blum N, Dahn RD, Begemann G, et al. Retinoic Acid Production by Endocardium and Epicardium Is an Injury Response Essential for Zebrafish Heart Regeneration. Dev Cell. 2011 Mar;20(3):397–404.

29. Jung HM, Castranova D, Swift MR, Pham VN, Venero Galanternik M, Isogai S, et al. Development of the larval lymphatic system in zebrafish. Dev Camb. 2017;144(11):2070–81.

30. Okuda KS, Astin JW, Misa JP, Flores MV, Crosier KE, Crosier PS. Lyve1 expression reveals novel lymphatic vessels and new mechanisms for lymphatic vessel development in zebrafish. Dev Camb. 2012;139(13):2381–91.

31. Leu DH, Draper BW. The ziwi promoter drives germline-specific gene expression in zebrafish. Dev Dyn. 2010 Aug 24;239(10):2714–21.

32. Ando K, Fukuhara S, Izumi N, Nakajima H, Fukui H, Kelsh RN, et al. Clarification of mural cell coverage of vascular endothelial cells by live imaging of zebrafish. Development. 2016 Jan 1;dev.132654.

33. Ellett F, Pase L, Hayman JW, Andrianopoulos A, Lieschke GJ. mpeg1 promoter transgenes direct macrophage-lineage expression in zebrafish. Blood. 2011 Jan 27;117(4):e49–56.

34. Davison JM, Akitake CM, Goll MG, Rhee JM, Gosse N, Baier H, et al. Transactivation from Gal4-VP16 transgenic insertions for tissue-specific cell labeling and ablation in zebrafish. Dev Biol. 2007;304(2):811–24.

35. Hao Y, Hao S, Andersen-Nissen E, Mauck WM, Zheng S, Butler A, et al. Integrated analysis of multimodal single-cell data. Cell. 2021 Jun;184(13):3573-3587.e29.

36. Satija R, Farrell JA, Gennert D, Schier AF, Regev A. Spatial reconstruction of single-cell gene expression data. Nat Biotechnol. 2015;33(5):495–502.

37. Shih YH, Portman D, Idrizi F, Grosse A, Lawson ND. Integrated molecular analysis identifies a conserved pericyte gene signature in zebrafish. Development. 2021 Dec 7;148(23):dev200189.

38. Padberg Y, Schulte-Merker S, van Impel A. The lymphatic vasculature revisited—new developments in the zebrafish. Methods Cell Biol. 2017;138:221–38.

39. Astin JW, Haggerty MJ, Okuda KS, Le Guen L, Misa JP, Tromp A, et al. Vegfd can compensate for loss of Vegfc in zebrafish facial lymphatic sprouting. Development. 2014;141(13):2680–90.

40. Bussmann J, Bos FL, Urasaki A, Kawakami K, Duckers HJ, Schulte-Merker S. Arteries provide essential guidance cues for lymphatic endothelial cells in the zebrafish trunk. Development. 2010 Aug 15;137(16):2653–7.

41. Cha YR, Fujita M, Butler M, Isogai S, Kochhan E, Siekmann AF, et al. Chemokine signaling directs trunk lymphatic network formation along the preexisting blood vasculature. Dev Cell. 2012;22(4):824–36.

42. Hogan BM, Bos FL, Bussmann J, Witte M, Chi NC, Duckers HJ, et al. Ccbe1 is required for embryonic lymphangiogenesis and venous sprouting. Nat Genet. 2009;41(4):396–8.

43. Nicenboim J, Malkinson G, Lupo T, Asaf L, Sela Y, Mayseless O, et al. Lymphatic vessels arise from specialized angioblasts within a venous niche. Nature. 2015;522(7554):56–61.

44. van Impel A, Zhao Z, Hermkens DM, Roukens MG, Fischer JC, Peterson-Maduro J, et al. Divergence of zebrafish and mouse lymphatic cell fate specification pathways. Development. 2014;141(6):1228–38.

45. Yaniv K, Isogai S, Castranova D, Dye L, Hitomi J, Weinstein BM. Imaging the developing lymphatic system using the zebrafish. In Chichester; New York; John Wiley; 1999; 2007. p. 139.

46. Küchler AM, Gjini E, Peterson-Maduro J, Cancilla B, Wolburg H, Schulte-Merker S. Development of the zebrafish lymphatic system requires VEGFC signaling. Curr Biol. 2006;16(12):1244–8.

47. Kaipainen A, Korhonen J, Mustonen T, van Hinsbergh VW, Fang GH, Dumont D, et al. Expression of the fms-like tyrosine kinase 4 gene becomes restricted to lymphatic endothelium during development. Proc Natl Acad Sci. 1995 Apr 11;92(8):3566–70.

48. Karkkainen MJ, Haiko P, Sainio K, Partanen J, Taipale J, Petrova TV, et al. Vascular endothelial growth factor C is required for sprouting of the first lymphatic vessels from embryonic veins. Nat Immunol. 2004 Jan;5(1):74–80.

49. Koltowska K, Lagendijk AK, Pichol-Thievend C, Fischer JC, Francois M, Ober EA, et al. Vegfc Regulates Bipotential Precursor Division and Prox1 Expression to Promote Lymphatic Identity in Zebrafish. Cell Rep. 2015;13(9):1828–41.

50. Villefranc JA, Nicoli S, Bentley K, Jeltsch M, Zarkada G, Moore JC, et al. A truncation allele in vascular endothelial growth factor c reveals distinct modes of signaling during lymphatic and vascular development. Development. 2013 Apr 1;140(7):1497–506.

51. Ferrara N, Gerber HP, LeCouter J. The biology of VEGF and its receptors. Nat Med. 2003 Jun 1;9(6):669–76.

52. Das RN, Tevet Y, Safriel S, Han Y, Moshe N, Lambiase G, et al. Generation of specialized blood vessels via lymphatic transdifferentiation. Nature. 2022 Jun 16;606(7914):570–5.

53. Fong GH, Rossant J, Gertsenstein M, Breitman ML. Role of the Flt-1 receptor tyrosine kinase in regulating the assembly of vascular endothelium. Nature. 1995 Jul;376(6535):66–70.

54. Bahrami N, Childs SJ. Pericyte biology in zebrafish. Adv Exp Med Biol. 2018;1109:33–51.

55. Robinson RS, Woad KJ, Hammond AJ, Laird M, Hunter MG, Mann GE. Angiogenesis and vascular function in the ovary. Reproduction. 2009 Dec;138(6):869–81.

56. Seynhaeve ALB, Oostinga D, van Haperen R, Eilken HM, Adams S, Adams RH, et al. Spatiotemporal endothelial cell – pericyte association in tumors as shown by high resolution 4D intravital imaging. Sci Rep. 2018 Dec;8(1):9596.

57. Svingen T, Koopman P. Building the mammalian testis: origins, differentiation, and assembly of the component cell populations. Genes Dev. 2013 Nov 15;27(22):2409–26.

58. Jokela H, Lokka E, Kiviranta M, Tyystjärvi S, Gerke H, Elima K, et al. Fetal-derived macrophages persist and sequentially maturate in ovaries after birth in mice. Eur J Immunol. 2020 Oct;50(10):1500–14.

59. Zhang Z, Huang L, Brayboy L. Macrophages: an indispensable piece of ovarian health. Biol Reprod. 2021 Mar 11;104(3):527–38.

60. Coveney D, Cool J, Oliver T, Capel B. Four-dimensional analysis of vascularization during primary development of an organ, the gonad. Proc Natl Acad Sci. 2008;105(20):7212–7.

61. Brown HM, Robker RL, Russell DL. Development and Hormonal Regulation of the Ovarian Lymphatic Vasculature. Endocrinology. 2010 Nov 1;151(11):5446–55.

62. Svingen T, François M, Wilhelm D, Koopman P. Three-Dimensional Imaging of Prox1-EGFP Transgenic Mouse Gonads Reveals Divergent Modes of Lymphangiogenesis in the Testis and Ovary. Mallo M, editor. PLoS ONE. 2012 Dec 20;7(12):e52620.

63. Wiens KM, Lee HL, Shimada H, Metcalf AE, Chao MY, Lien CL. Platelet-Derived Growth Factor Receptor β Is Critical for Zebrafish Intersegmental Vessel Formation. Hendricks M, editor. PLoS ONE. 2010 Jun 25;5(6):e11324.

64. Bower NI, Koltowska K, Pichol-Thievend C, Virshup I, Paterson S, Lagendijk AK, et al. Mural lymphatic endothelial cells regulate meningeal angiogenesis in the zebrafish. Nat Neurosci. 2017;20(6):774–83.

65. Redmer DA, Reynolds LP. Angiogenesis in the ovary. Rev Reprod. 1996;1(3):182–92.

66. Israely T, Dafni H, Granot D, Nevo N, Tsafriri A, Neeman M. Vascular remodeling and angiogenesis in ectopic ovarian transplants: A crucial role of pericytes and vascular smooth muscle cells in maintenance of ovarian grafts. Biol Reprod. 2003;68(6):2055–64.

67. Chiaverina G, di Blasio L, Monica V, Accardo M, Palmiero M, Peracino B, et al. Dynamic Interplay between Pericytes and Endothelial Cells during Sprouting Angiogenesis. Cells. 2019;8(9):1–13.

68. Kofler N, Naiche LA, Zimmerman LD, Kitajewski JK. Inhibition of Jagged-Specific Notch Activation Reduces Luteal Angiogenesis and Causes Luteal Hemorrhaging of Hormonally Stimulated Ovaries. ACS Pharmacol Transl Sci. 2019;2(5):325–32.

69. Hall AP, Ashton S, Horner J, Wilson Z, Reens J, Richmond GHP, et al. PDGFR Inhibition Results in Pericyte Depletion and Hemorrhage into the Corpus Luteum of the Rat Ovary. Toxicol Pathol. 2016;44(1):98–111.

70. Hess KA, Chen L, Larsen WJ. The ovarian blood follicle barrier is both charge- and size-selective in mice. Biol Reprod. 1998;58(3):705–11.

71. Siu MKY, Cheng CY. The Blood-Follicle Barrier (BFB) in disease and in ovarian function. Adv Exp Med Biol. 2013;763:186–92.

72. Gaengel K, Niaudet C, Hagikura K, Laviña B, Muhl L, Hofmann JJ, et al. The Sphingosine-1-Phosphate Receptor S1PR1 Restricts Sprouting Angiogenesis by Regulating the Interplay between VE-Cadherin and VEGFR2. Dev Cell. 2012 Sep;23(3):587–99.

73. Yanagida K, Liu CH, Faraco G, Galvani S, Smith HK, Burg N, et al. Size-selective opening of the blood–brain barrier by targeting endothelial sphingosine 1–phosphate receptor 1. Proc Natl Acad Sci. 2017 Apr 25;114(17):4531–6.

74. Wang X, Qiu Z, Dong W, Yang Z, Wang J, Xu H, et al. S1PR1 induces metabolic reprogramming of ceramide in vascular endothelial cells, affecting hepatocellular carcinoma angiogenesis and progression. Cell Death Dis. 2022 Sep 6;13(9):768.

75. Pascuali N, Scotti L, Oubiña G, de Zúñiga I, Gomez Peña M, Pomilio C, et al. Platelet-derived growth factor B restores vascular barrier integrity and diminishes permeability in ovarian hyperstimulation syndrome. Mol Hum Reprod. 2020 Aug 1;26(8):585–600.

627 76. Di Pietro M, Pascuali N, Parborell F, Abramovich D. Ovarian angiogenesis in polycystic
628 ovary syndrome. Reproduction. 2018;155(5):R199–209.

629 77. Zaidi J, Campbell S, Pittrof R, Kyei-Mensah A, Shaker A, S.Jacobs H, et al. Contraception:
630 Ovarian stromal blood flow in women with polycystic ovaries—a possible new marker for
631 diagnosis? Hum Reprod. 1995 Aug 1;10(8):1992–6.

632 78. Yan YL, Desvignes T, Bremiller R, Wilson C, Dillon D, High S, et al. Gonadal soma controls
633 ovarian follicle proliferation through Gsdf in zebrafish. Dev Dyn. 2017 Nov;246(11):925–45.

634 79. Fantin A, Vieira JM, Gestri G, Denti L, Schwarz Q, Prykhozhij S, et al. Tissue macrophages
635 act as cellular chaperones for vascular anastomosis downstream of VEGF-mediated
636 endothelial tip cell induction. Blood. 2010 Aug 5;116(5):829–40.

637 80. Eubank TD, Galloway M, Montague CM, Waldman WJ, Marsh CB. M-CSF Induces Vascular
638 Endothelial Growth Factor Production and Angiogenic Activity From Human Monocytes 1. J
639 Immunol. 2003 Sep 1;171(5):2637–43.

640 81. Rymo SF, Gerhardt H, Wolfhagen Sand F, Lang R, Uv A, Betsholtz C. A Two-Way
641 Communication between Microglial Cells and Angiogenic Sprouts Regulates Angiogenesis
642 in Aortic Ring Cultures. PLOS ONE. 2011 Jan 10;6(1):e15846.

643 82. Martin P, Gurevich DB. Macrophage regulation of angiogenesis in health and disease. Spec
644 Issue Muscle Growth Regen Kathryn Wagner Spec Issue Role Macrophages Tissue
645 Homeost Benedicte Chazaud. 2021 Nov 1;119:101–10.

646 83. Sunderkötter C, Goebeler M, Schulze-Osthoff K, Bhardwaj R, Sorg C. Macrophage-derived
647 angiogenesis factors. Pharmacol Ther. 1991 Jan 1;51(2):195–216.

648 84. Wu R. Macrophage contributions to ovarian function. Hum Reprod Update. 2004 Mar
649 1;10(2):119–33.

650 85. Ono Y, Nagai M, Yoshino O, Koga K, Nawaz A, Hatta H, et al. CD11c+ M1-like
651 macrophages (MΦs) but not CD206+ M2-like MΦ are involved in folliculogenesis in mice
652 ovary. Sci Rep. 2018 Dec;8(1):8171.

653

654 **Figure legends**:

655

656 **Figure 1. Vascular Endothelial Cells in the Bipotential Gonad. (A-H)** Representative images

657 showing the defined 3 categories for describing the relationship between vascular endothelial

658 cells and germ cells in the biopotential gonad: “No Contact” (**A**), “proximal” (**B-C**; open

659 arrowhead), and “Contact” (**D-E**; red arrow). All images are oriented with anterior (A) to the left

660 and posterior (P) to the right. (**F**) The relationship between the vascular endothelial cells and the

germ cells was categorized in individuals from multiple independent spawning events and correlated with age (see Supplemental Table S1). Vascularization of the gonad occurs in most individuals by 20 dpf. (**G**) Standard length is a more accurate measure of development. Most fish had vascularized gonads when they reached a standard length of 7.21±0.666mm. (**H**) The main vessel supplying the gonad with blood, the gonadal artery (white arrowheads), originates from the swim bladder artery (red arrowheads). (**I**) A schematic representing the GA and SBA in the context of the body cavity. VEC = Vascular Endothelial Cell, AC = Anterior Chamber, SBA = Swim Bladder Artery, PD = Pneumatic Duct, AC = Anterior Chamber, PC = Posterior Chamber. Scale = 100 μm.

Figure 2. The primary stromal cell populations are present in the gonad when fish reach a standard length of approximately 7mm. (**A**) At each age, individuals from multiple spawns were collected to determine if there was contact between the stromal cell of interest and the germ cells. Vascular endothelial cells (red circle), Lymphatic endothelial cells (green triangle), Pericytes (blue square), and macrophage (purple diamonds) all reach the gonad at approximately the same time, 15-20 dpf. (**B**) Each fish was measured before dissection for the standard length which corresponds to its development. The full list of replicates, individuals, average length, and observations can be found in **Supplemental Table S1**.

Figure 3. Endothelial gene expression in 40 dpf ovary. (A) Expression of vascular endothelial cell genes *kdrl, fli1*, and *flt1* occurs in a majority of the endothelial cells. (**B**) lymphatic endothelial genes *lyve1b*, *flt4*, and *prox1* are expressed in a smaller subset of cells. (**C**) There is no overlap in expression of *kdrl* (red) and *lyve1b* (green) by single-cell sequencing, expression overlap is shown in yellow as demonstrated in the fourth pane. (**D**) There is overlap in expression of *flt4* (red) and *lyve1b* (green) suggesting that lymphatic endothelial cells originate canonically.

687

688 **Figure 4. *kdrl* and *mrc1a* are co-expressed in the 20 dpf ovary.** (**A**) Maximum intensity
689 projection of the 20 dpf gonad (germ cells = blue, gonad outlined) showing overlap in *kdrl*
690 (magenta) and *mrc1a* (green) expression. (**B**) Single channel showing *kdrl* expression alone
691 suggests that *kdrl* is expressed in all cells. (**C**) Single channel showing *mrc1a* expression is
692 inversely correlate with the strength of *kdrl* expression. (**D**) Orthogonal slice of the maximum
693 intensity projection shows that the expression of both markers is overlapping within cells. (**E**)
694 Co-localization analysis of the cells circled in red in (**F**) showing expression of *kdrl* and *mrc1a* is
695 highly correlated. Scale = 20 μm.

696

697 **Figure 5. The *pdgfrb*+ expression domain encompasses multiple ovarian stromal cell**
698 **types**. In the embryo, cluster 39 (pink) represents a subset of *pdgfrb*+ cells (blue) that are more
699 specific to pericytes. In the ovary, *pdgfrb* is expressed in all ovarian stromal cells (purple), but a
700 subset have more specific pericyte gene expression (yellow).

701

702 **Figure 6. *pdgfrb* positive cells elongate prior to vascular endothelial cells**. Pericytes,
703 labeled with *pdgfrb:EGFP* (green) extend protrusions (white arrows) from existing vessels into
704 the gonad (blue, outlined in white), likely following the endothelial tip cell (magenta). Scale = 20
705 μm

706

707 **Figure 7. Tissue-resident macrophage engulf cells during gonad differentiation.** (**A**)
708 Macrophage can be found in contact with germ cells as early as 12 dpf. (**B**) At 20 dpf,
709 macrophage are abundant in the gonad. (**C**) Macrophage (magenta) are observed removing
710 oocyte material (green) and DNA (white) from the former bipotential gonad (white arrowheads).
711 (**D**) *mpeg1:GAL4; UAS:Kaede* expressing macrophage were photoconverted from green to red

712 (pseudocolored magenta) at 12 dpf. 24 hours after conversion both green and red macrophage
713 could be found in the gonad (blue arrow, outlined). (**E**) Some macrophage in the gonad were
714 only magenta (red arrowhead), indicating that they are resident to the gonad during this period.
715 (**F**) In the green channel, we can observe that some macrophage migrate to the gonad within
716 the 24 hour window post-photoconversion (green arrows). Scale listed.
717

718 **Figures**:

719 **Figure 1.**

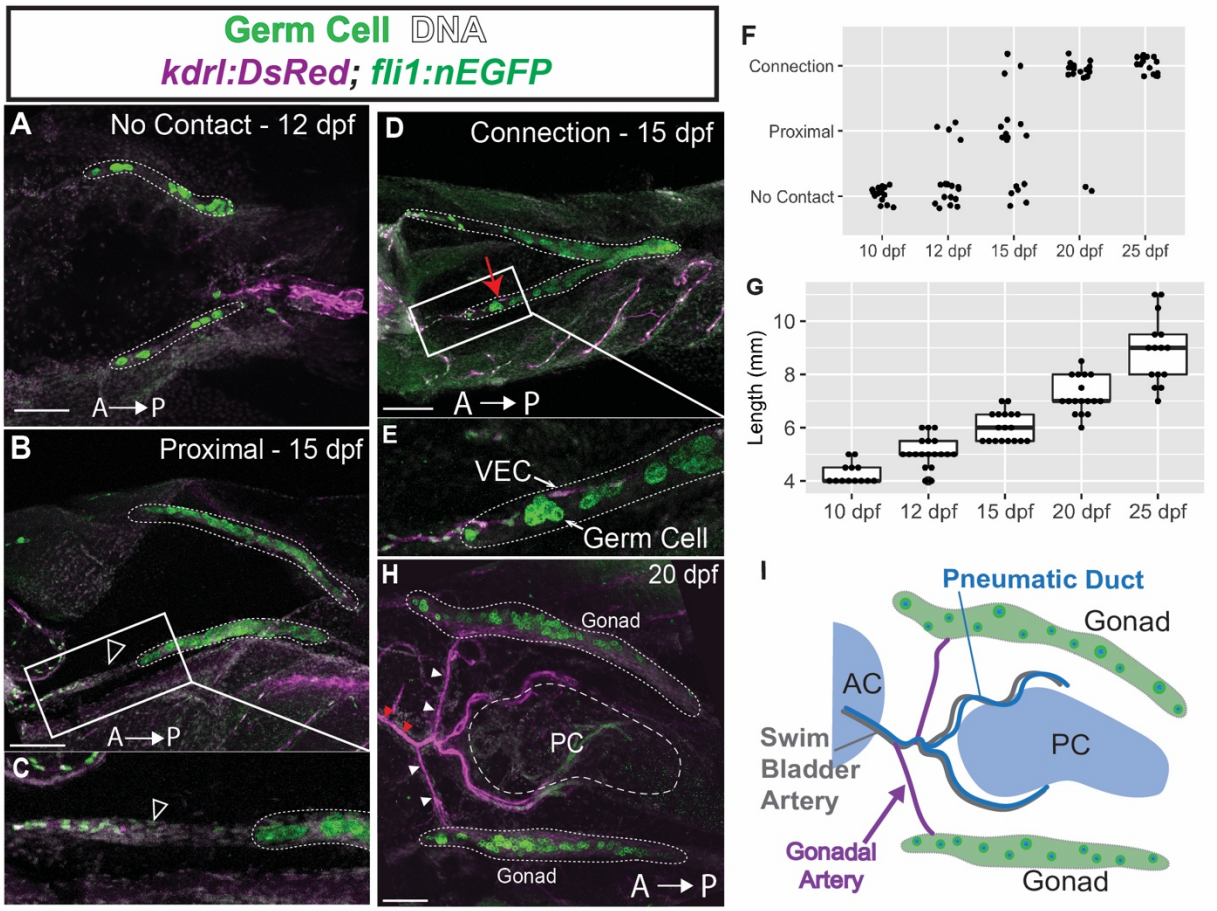

720

721

722 **Figure 2**.

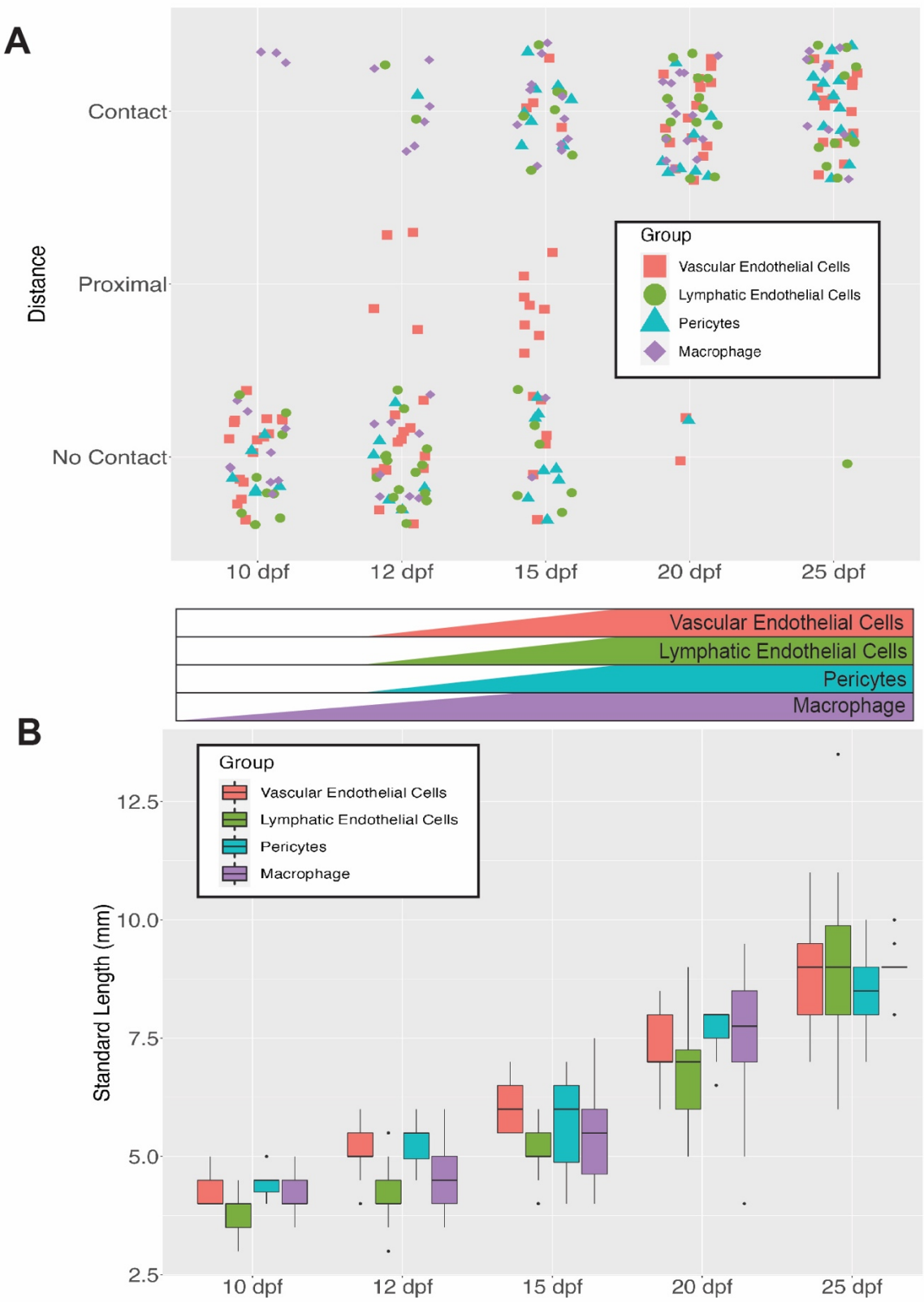

723

724 **Figure 3.**

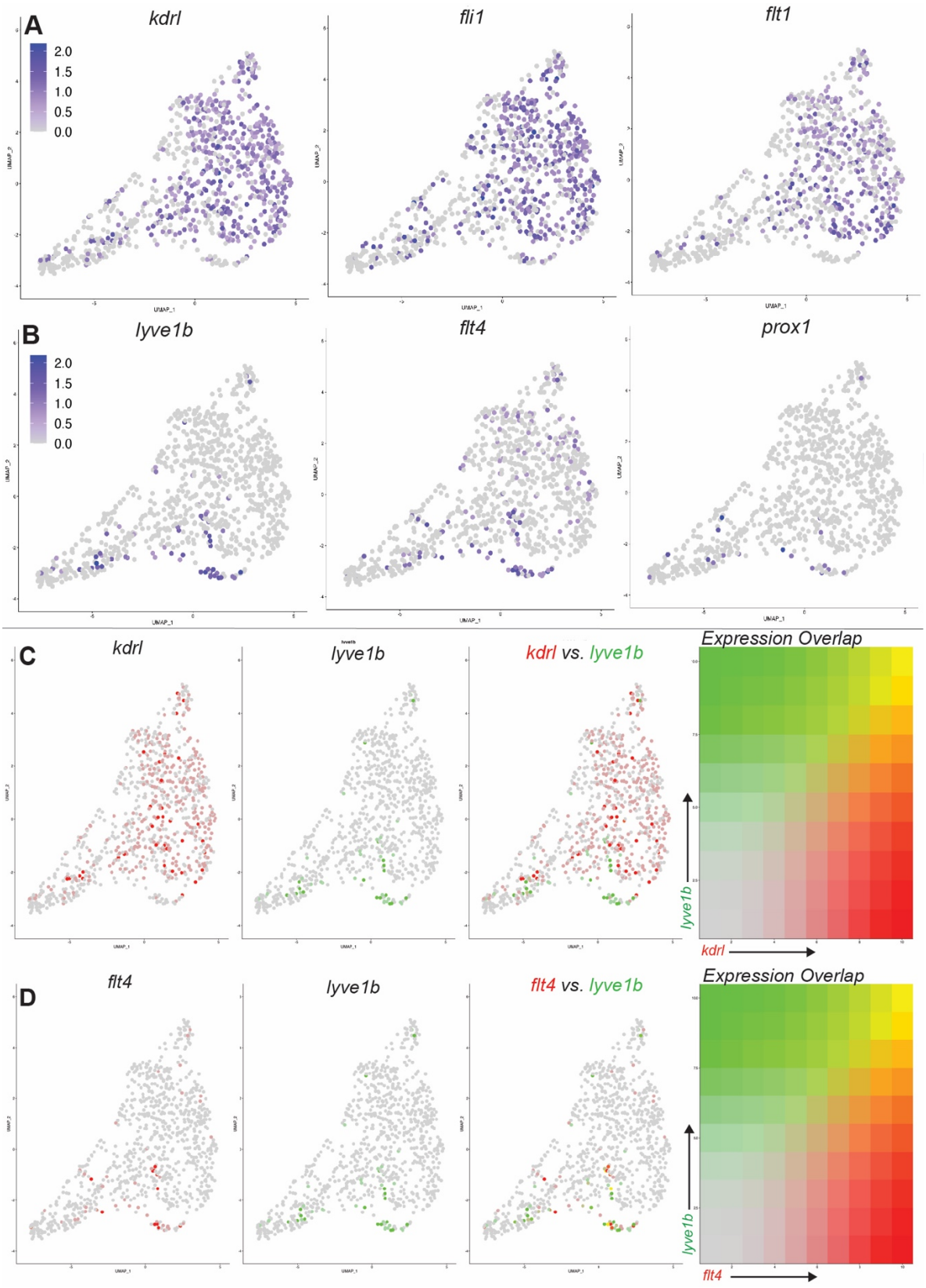

725

Figure 4.

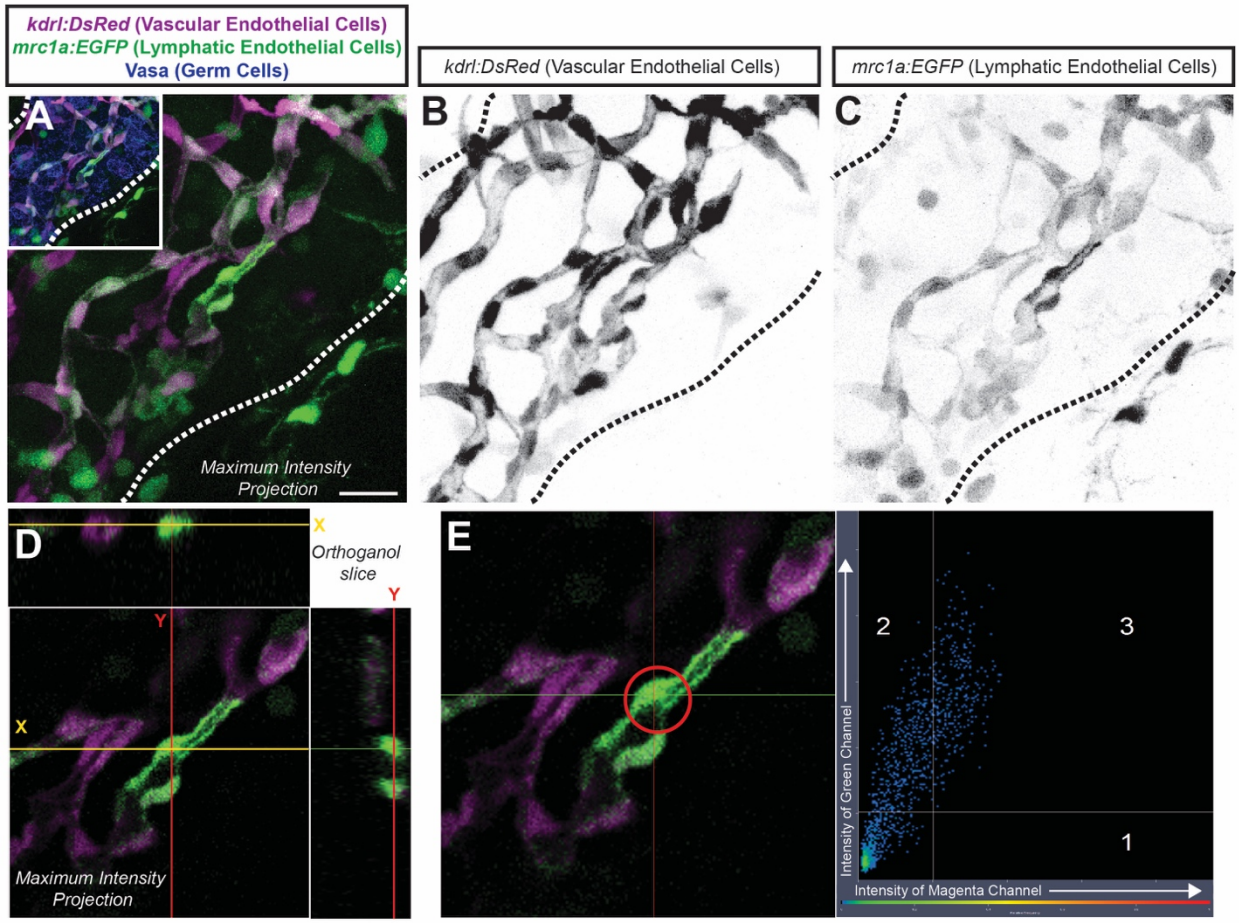

729 **Figure 5.**

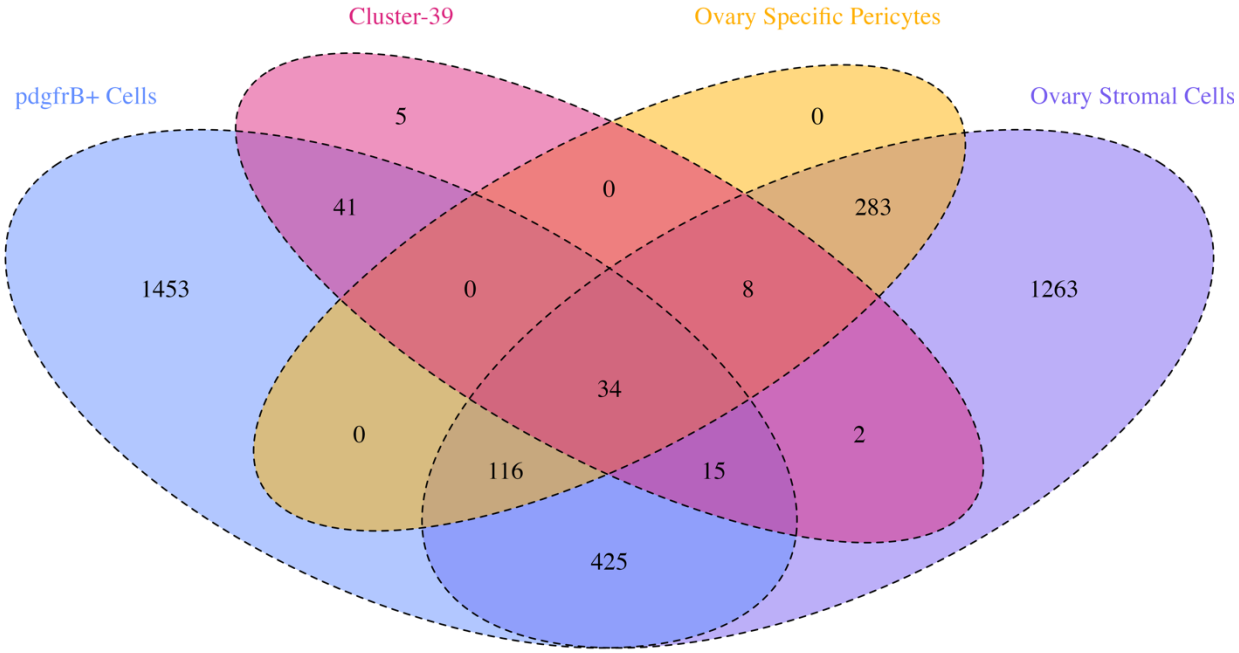

730

731

Figure 6.

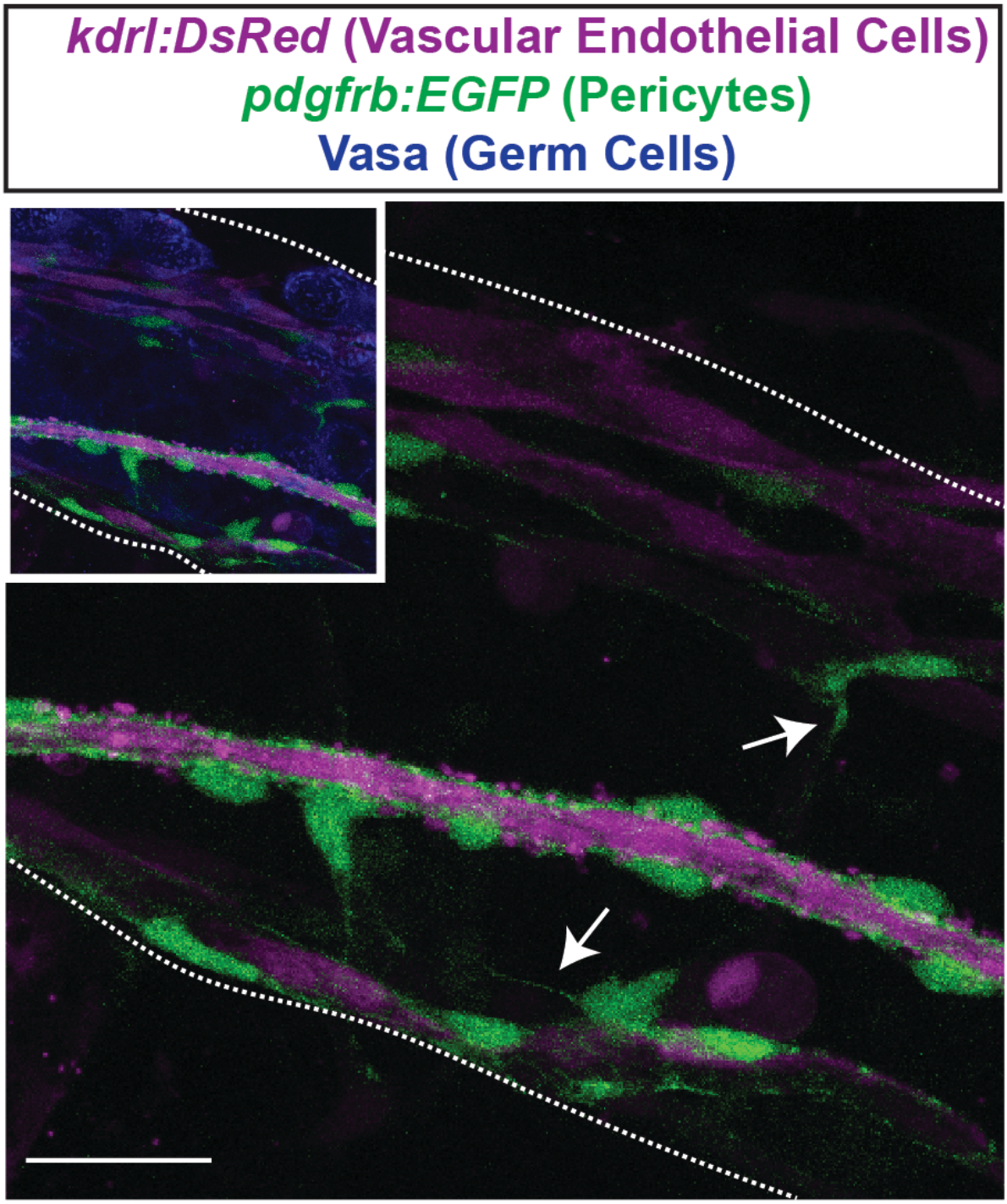

736 **Figure 7.**

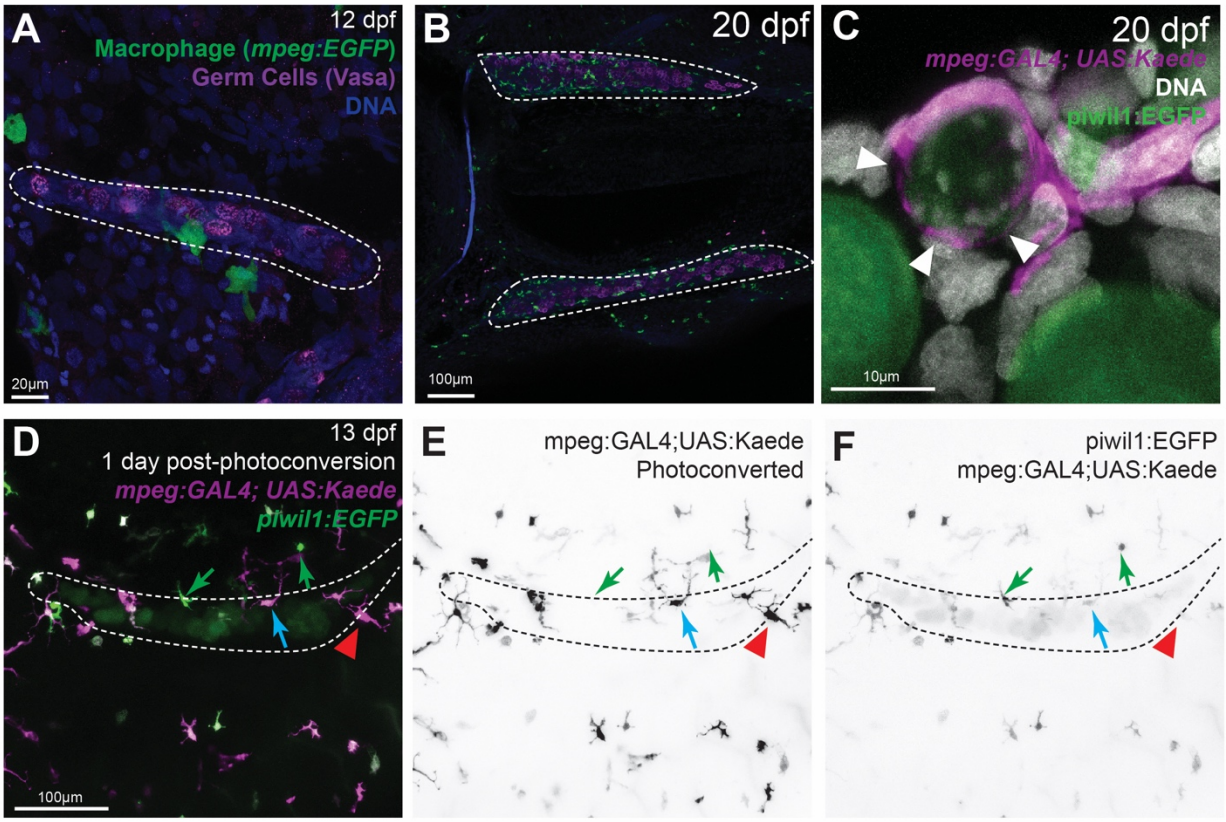

737